Journal of Hazardous Materials 178 (2010) 658–664

Contents lists available at ScienceDirect

Journal of Hazardous Materials

journal homepage: www.elsevier.com/locate/jhazmat

Preparation of highly ordered cubic NaA zeolite from halloysite mineral for adsorption of ammonium ions

Yafei Zhao [a], Bing Zhang [a,b,*], Xiang Zhang [a], Jinhua Wang [a], Jindun Liu [a], Rongfeng Chen [b]

[a] School of Chemical Engineering, Zhengzhou University, Zhengzhou 450001, PR China
[b] Henan Academy of Sciences, Zhengzhou 450002, PR China

ARTICLE INFO

Article history:
Received 9 October 2009
Received in revised form 27 January 2010
Accepted 27 January 2010
Available online 2 February 2010

Keywords:
NaA zeolite
Hydro-thermal method
Ammonium ions
Halloysite mineral
Adsorption

ABSTRACT

Well-ordered cubic NaA zeolite was first synthesized using natural halloysite mineral with nanotubular structure as source material by hydro-thermal method. SEM and HRTEM images indicate that the synthesized NaA zeolite is cubic-shaped crystal with planar surface, well-defined edges and symmetrical and uniform pore channels. The adsorption behavior of ammonium ions (NH_4^+) from aqueous solution onto NaA zeolite was investigated as a function of parameters such as equilibrium time, pH, initial NH_4^+ concentration, temperature and competitive cations. The Langmuir and Freundlich adsorption models were applied to describe the equilibrium isotherms. A maximum adsorption capacity of 44.3 mg g^{-1} of NH_4^+ was achieved. The regeneration and reusable ability of this adsorbent was evaluated, and the results indicated that the recovered adsorbent could be used again for NH_4^+ removal with nearly constant adsorption capacity. Thermodynamic parameters such as change in free energy (ΔG^0), enthalpy (ΔH^0) and entropy (ΔS^0) were also determined, which indicated that the adsorption was a spontaneous and exothermic process at ambient conditions. Compared with other adsorbents, the as-synthesized NaA zeolite displays a faster adsorption rate and higher adsorption capacity, which implies potential application for removing NH_4^+ pollutants from wastewaters.

1. Introduction

Recently, people pay more attention on removal of ammonium ions (NH_4^+) from wastewaters because accumulation of NH_4^+ in water will cause a sharp decrease of dissolved oxygen and obvious toxicity on aquatic organisms [1]. Various methods including physical, chemical and biological methods have been used for NH_4^+ removal [2–4]. Among these methods available for NH_4^+ removal, adsorption is considered to be an attractive and effective technique [5–8]. Activated carbon was widely recognized as effective material for removing NH_4^+ from wastewaters [9,10]. However, its relatively high price restricts the practical industrial application. Zeolite is a promising alternative because of its low cost, selectivity and compatibility with the natural environment. Zeolite is framework aluminosilicate with pore dimensions of molecular sizes generated by corner-sharing Al^{3+} and Si^{4+} oxygen tetrahedra. The aluminum ion is small enough to occupy the position in the center of the tetrahedron of four oxygen atoms, and the isomorphous replacement of Si^{4+} by Al^{3+} produces a negative charge in the lattice. The net negative charge is balanced by the exchangeable cation (sodium, potassium and/or calcium, etc.). These exchangeable cations give rise to the ion-exchange or adsorption capability with NH_4^+.

Natural zeolite from different deposits has been widely reported as adsorbent for NH_4^+ removal in wastewaters [11–14]. Due to synthetic zeolite having uniform micropore structure and high surface area, it usually has a higher adsorption capability compared with natural zeolite. Therefore, in order to obtain low-cost and effective synthetic zeolite, many researchers have investigated the synthesis of zeolite from coal fly ash, asbestos, fly ash, metakaolinite, chrysotile and rice husk etc. [15–20]. However, in many of these studies, the total conversion time was generally long (24–72 h or more); the synthesis temperature was high (363–498 K); and the synthetic zeolite products still contained a significant amount of residual raw materials and/or other phases. The presence of non-zeolitic phases in the converted products limits the cation exchange capacity of the products and greatly reduces the applicability of synthetic zeolite. Therefore, developing effective, high adsorption capacity and low-cost synthetic zeolite for NH_4^+ removal continues to be a great challenge.

Halloysite is a two-layered aluminosilicate clay mineral, consisting of one alumina octahedron sheet and one silica tetrahedron sheet in a 1:1 stoichiometric ratio, and it is available in abundance in some countries such as China, America, Brazil and France [21,22]. Halloysite has a similar structure and composition as kaolinite, but the unit layers are separated by a monolayer of water molecules.

* Corresponding author at: School of Chemical Engineering, Zhengzhou University, Zhengzhou 450001, PR China. Tel.: +86 371 67781724; fax: +86 371 67781724.
E-mail address: zhangb@zzu.edu.cn (B. Zhang).

0304-3894/$ – see front matter © 2010 Elsevier B.V. All rights reserved.
doi:10.1016/j.jhazmat.2010.01.136

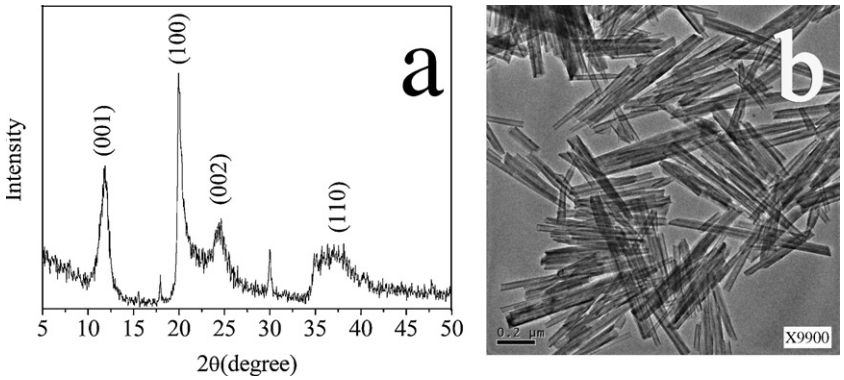

Fig. 1. The characterization of halloysite (a) XRD pattern and (b) TEM micrograph.

Due to its high surface area and hollow structure, halloysite could be used as promising material with high reactivity to synthesize highly pure zeolite. Up to now, we have found no studies on the synthesis of zeolite from halloysite.

Herein, in this paper, we introduce halloysite mineral as a source material to prepare pure, single phase, highly crystalline NaA zeolite by hydro-thermal method under lower temperature (363 K) and shorter conversion time (5 h). Meanwhile, the prepared NaA zeolite was used as adsorbent to remove NH_4^+ from aqueous solution. Parameters affecting the adsorption such as equilibrium time, pH, initial NH_4^+ concentration, temperature and competitive cations were investigated, and the isotherms and thermodynamics were also studied. In addition, the regeneration and reusable ability of NaA zeolite were evaluated. The results indicated that the prepared NaA zeolite exhibited fast adsorption rate, high adsorption capacity and the recovered adsorbent can be used again for NH_4^+ removal.

2. Experimental and methods

2.1. Raw materials

Natural halloysite mineral, used as silicon and aluminum sources in this work, was obtained from clay minerals in Henan Province, China. The composition of halloysite was analyzed by chemical method. The analysis result indicates it contains 46.15% SiO_2, 38.70% Al_2O_3, 0.033% MgO, 0.192% CaO, 0.05% Fe_2O_3, 0.03% K_2O, 0.04% Na_2O, 0.004% TiO_2 and 14.60% loss on ignition.

Fig. 1 displays the typical XRD pattern and TEM image of the natural halloysite mineral. Fig. 1a shows that the diffraction peaks of original mineral can be indexed to the hexagonal structured $Al_2Si_2O_5(OH)_4$, which are in agreement with the reported values of Halloysite-7 Å with the lattice constants $a = 5.13$, $c = 7.16$ (JCPDS Card No. 29-1487). The diffraction peak (0 0 1) at 12.1° in 2θ, corresponding to a basal spacing of 0.72 nm, which further identifies the mineral as halloysite-7 Å. The significant broadening of the diffraction peaks are ascribed to the very small crystallite size. Fig. 1b shows that the halloysite particles have a cylindrical shape and contain a transparent central area that runs longitudinally along the cylinder, indicating that the nanotubular particles are hollow and open-ended. The morphological parameters of the halloysite sample, measured from the TEM image, are an average length of 0.5–1 μm, a diameter in the range of 20–50 nm, and an average pore diameter of 10–40 nm. The small crystallite size and hollow structure endow halloysite mineral with a high specific surface area of about 79.62 $m^2\,g^{-1}$, which is favourable for hydro-thermal reaction.

Other inorganic chemicals used in the study, such as ammonium chloride (NH_4Cl), sodium chloride (NaCl), sodium hydroxide (NaOH) and hydrochloric acid (HCl) were all analytical grade reagents. A stock solution (1000 mg L^{-1}) was prepared by dissolving NH_4Cl in distilled water; desired concentrations were obtained when needed by diluting the stock solution with distilled water. HCl and NaOH solutions were used for pH adjustment.

2.2. Preparation of NaA zeolite

NaA zeolite was prepared using alkaline fusion followed by hydro-thermal treatment method. 2 g of halloysite powder was placed in a Ni crucible and fused with 2.6 g NaOH powder at 673 K for 2 h to promote their reactivity. The fused mass obtained was cooled and mixed with deionized water (38 mL) by magnetic stirring for 30 min until the reaction gel was homogenized. The aluminosilicate gel was aged for 2 h at 313 K in the sealed Teflon reactor to rearrange the reactant for forming nuclei. After that, the mixture was crystallized at 363 K for 5 h under static condition. Solid powder was filtered-off, washed, dried at 383 K for 12 h and the product was obtained.

2.3. Characterization

The as-prepared NaA zeolite was characterized by XRD, FTIR, SEM and TEM. XRD pattern was obtained using a Philips X Pert-Pro diffractometer with Cu Kα (λ = 0.154 nm) radiation operating at 35 kV and 25 mA and a step width of 0.04°. Fourier transformed infrared spectroscopy (FTIR) was recorded on a Nicolet Nexus 470 FTIR spectrometer in the range 400–4000 cm^{-1}. Field emission scanning electron microscopy (FE-SEM) was performed using a JSM-6700F SEM (JEOL), operating in backscatter mode at 20 kV accelerating voltage. Transmission electron microscopy (TEM) and high-resolution transmission electron microscopy (HRTEM) were obtained with a FEITECNA1G2 electron microscope operating at an acceleration voltage of 120 kV.

2.4. NH_4^+ adsorption experiments

The batch experiments were carried out in stopper conical flasks containing 50 mL varying initial concentration of NH_4^+ solutions and adsorbent dose. Then the samples were agitated on a thermostated shaker with a shaking of 180 rpm at 288–338 K. On reaching equilibrium the adsorbent was eliminated by centrifugation at 3000 rpm and then filtered with 0.45 μm membranes. The initial and final ammonium concentrations remaining in solutions were analyzed using a UV spectrophotometer (Shimadzu, UV-3000) by monitoring the absorbance changes at a wavelength of maximum absorbance (420 nm). The removal efficiency (R, %), the amount of ammonium adsorbed at time t (q_t, mg g^{-1}) and at equilibrium (q_e, mg g^{-1}) was calculated by using the following

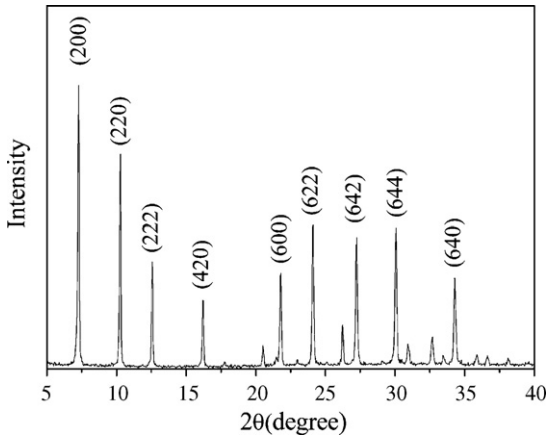

Fig. 2. XRD pattern of synthesized NaA zeolite obtained by halloysite.

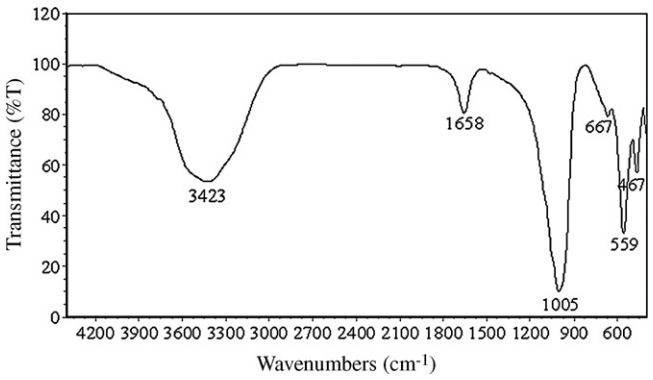

Fig. 3. FT-IR spectra of synthesized NaA zeolite obtained by halloysite.

equations, respectively.

$$R = \frac{100(C_0 - C_e)}{C_0} \quad (1)$$

$$q_t = \frac{(C_0 - C_t)V}{M} \quad (2)$$

$$q_e = \frac{(C_0 - C_e)V}{M} \quad (3)$$

where C_0, C_t and C_e (mg L^{-1}) are the initial, t time and equilibrium concentrations of ammonium solution, respectively; V (L) is the volume of ammonium solution and M (g) is the weight of NaA zeolite.

3. Results and discussion

3.1. Characterization of NaA zeolite

Fig. 2 shows the XRD pattern of the product. The typical diffraction peaks corresponding to halloysite remarkably disappear. All XRD peaks agree well with the characteristic peaks of zeolite NaA ($Na_{96}Al_{96}Si_{96}O_{384}{\cdot}216H_2O$) by comparing the d-values of the products obtained with JCPDS data of card No. 39-0222. No additional peaks are observed, indicating the crystallization of pure-form NaA zeolite. The XRD of the crystals has a low background, strong intensities and sharp peaks, indicating the as-synthesized NaA zeolite crystals are perfect.

FTIR spectrum is shown in Fig. 3. The typical bands of NaA zeolite representing the asymmetric and symmetric stretch (1005 cm^{-1}), double rings (559 cm^{-1}) and T (Al, Si)–O bend (667 and 467 cm^{-1}) are observed. The band at about 1658 cm^{-1} is attributed to the presence of the H_2O mode and incomplete dehydration of the zeolite samples. Moreover, the observed single strong band at 3423 cm^{-1} ascribed to the presence of hydroxyls. All the characteristic IR bands of the NaA zeolite are similar to the zeolite LTA synthesized from kaolinite [23].

Cubic crystalline structure with well defined edge of the NaA zeolite particles can be readily observed in SEM images (Fig. 4). The particle size and average width of the product can be estimated, 1–2 μm and 1.5 μm, respectively. TEM and HRTEM images of sample are shown in Fig. 5. According to TEM image (Fig. 5a), particle size of the synthesized zeolite has been estimated less than 2 μm and the crystals are beveled cubes. The lattice fringe can be clearly seen from the HRTEM image (Fig. 5b), implying the good crystallization of the NaA zeolite. Calculation shows a lattice spacing of 0.4 nm, which corresponds to the pore diameter of NaA zeolite. The symmetrical and uniform pore channels provide huge surface of active sites and ions can penetrate into the pore channels or adsorb on the surface easily. So it has significant potential application for the adsorption of harmful ions.

3.2. Adsorption rate

In order to determine the time required for the NH_4^+–NaA zeolite system to reach equilibrium, 50 mL 100 mg L^{-1} NH_4^+ solution was shaken with 0.5 g NaA zeolite under 288 K. The equilibrium studies were performed at the selected interval of time ranging from 5 to 180 min. The result is illustrated in Fig. 6. NaA zeolite exhibits rapid adsorption rate and reaches adsorption equilibrium within 15 min. The rate of NH_4^+ ions removal by NaA zeolite is high in the initial 10 min, but thereafter the rate significantly reduces and eventually equilibrates. The change in the rate of NH_4^+ ions removal might be due to the fact that initially all adsorbent sites are vacant and the solute concentration gradient is high. Afterwards the NH_4^+ ions uptake rate by the NaA zeolite decreases significantly due to decrease in adsorption sites. Saltali et al. [12] also found

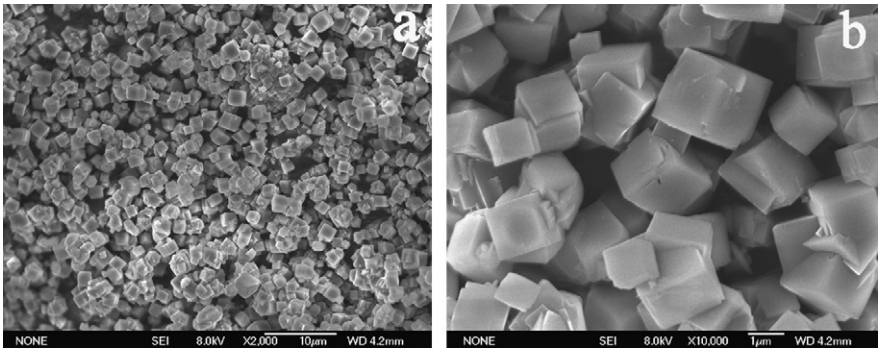

Fig. 4. SEM images of synthesized NaA zeolite obtained by halloysite (a) ×2000 and (b) ×10000.

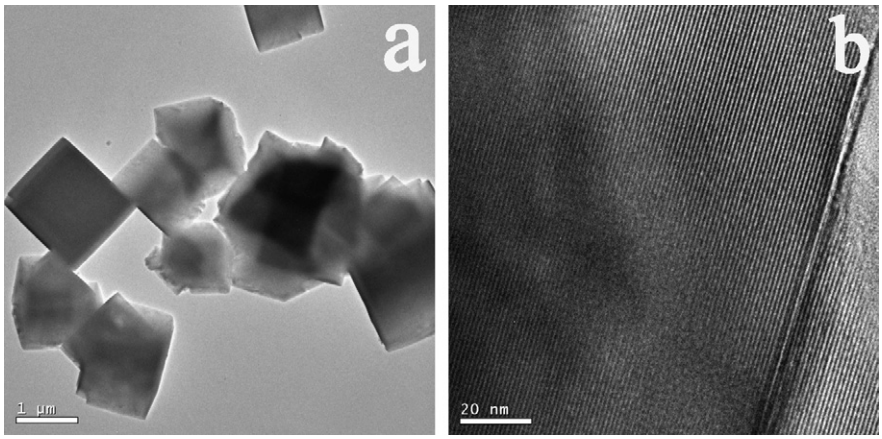

Fig. 5. TEM and HRTEM micrographs of synthesized NaA zeolite obtained by halloysite (a) TEM and (b) HRTEM.

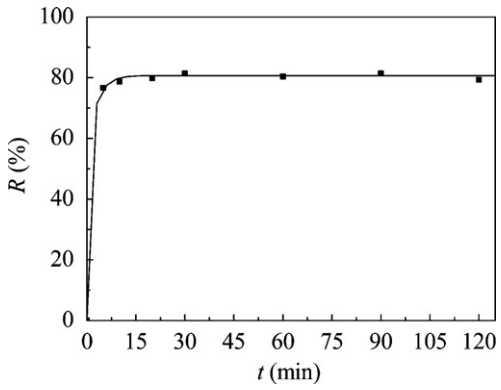

Fig. 6. Effect of contact time for NH_4^+ adsorption on synthesized NaA zeolite at 288 K.

that ammonium uptake by zeolite was a fast process that occurred within 15 min. As seen from these values, there is no significant difference in the removal efficiency determined after 30 min and after 180 min. On the basis of these results, a 30 min shaking period was selected for all further studies.

3.3. Effect of initial pH

Effect of initial pH was investigated at pH ranging from 4 to 10. The pH values were adjusted by 0.1 mol L^{-1} HCl and 0.1 mol L^{-1} NaOH solutions. In this study, 50 mL 100 mg L^{-1} NH_4^+ solution was agitated with 0.2 g NaA zeolite at 288 K. The result is given in Fig. 7. The maximum removal efficiency of NH_4^+ is achieved when the experiment is operated at pH 7.0. pH has an obvious impact on NH_4^+ removal by NaA zeolite since it can influence the character of the ammonium ions. At lower pH, the NH_4^+ ions have to compete with hydrogen ions among the adsorption sites; however, when the pH is higher than 7.0, the ionized NH_4^+ is gradually transformed to non-ionized forms NH_3, which is unfavorable for adsorption on the surface of NaA zeolite [8]. As the initial pH of NH_4^+ solution is near 7.0, the pH of solution was not adjusted in the next experiments.

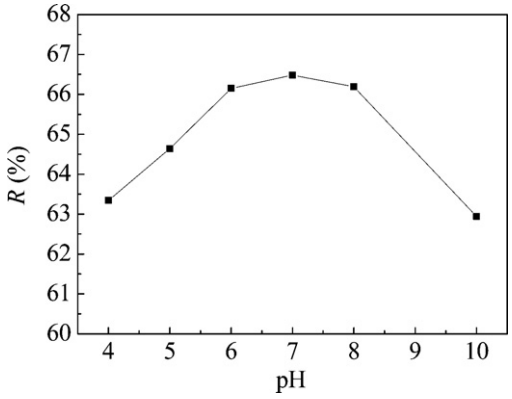

Fig. 7. Effect of pH values for NH_4^+ adsorption on synthesized NaA zeolite at 288 K.

3.4. Effect of temperature

The effect of temperature was studied at 288–338 K with 50 mL 100 mg L^{-1} NH_4^+ solution and 0.2 g NaA zeolite. The result is shown in Fig. 8. The adsorption capacity of NH_4^+ onto NaA zeolite was found to decrease with increase in temperature, thereby indicating the process was exothermic. This may be due to a tendency for the NH_4^+ ions to escape from the solid phase to the bulk phase with an increase in temperature of the solution [12].

3.5. Effect of initial NH_4^+ concentration

The effect of initial NH_4^+ concentration was studied at different initial NH_4^+ concentrations in the range of 10–300 mg L^{-1} at 288 K with 0.2 g NaA zeolite, respectively. The result is shown in Fig. 9. It is observed that NH_4^+ adsorption capacity increases with increasing initial NH_4^+ concentration in solution. This can be attributed to the fact that higher concentrations result in a higher solute gradient, providing the necessary driving force for NH_4^+ ions to replace cations in the media framework. The results, presented in Fig. 9, also show a decrease in the NH_4^+ removal efficiency when the

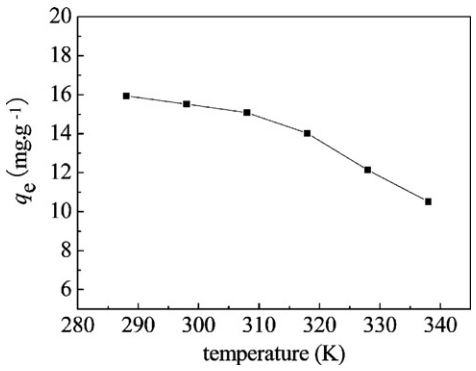

Fig. 8. Effect of temperature for NH_4^+ adsorption on synthesized NaA zeolite.

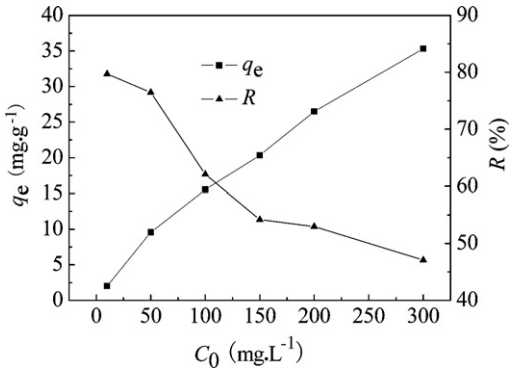

Fig. 9. Effect of NH_4^+ initial concentration for adsorption on synthesized NaA zeolite at 288 K.

NH_4^+ concentration in solution increases, due to saturation of the adsorbent.

3.6. NH_4^+ adsorption isotherms study

Adsorption isotherms are essential for the description of how NH_4^+ interacts with NaA zeolite and are useful to optimize the use of NaA zeolite as adsorbent. Both Langmuir and Freundlich models are used for the evaluation of experimental results.

The linear form of Langmuir equation is given as:

$$\frac{C_e}{q_e} = \frac{1}{q_{max}K_L} + \frac{C_e}{q_{max}} \quad (4)$$

where q_e (mg g^{-1}) is the equilibrium amount of NH_4^+ adsorption by NaA zeolite, C_e (mg L^{-1}) is the equilibrium NH_4^+ concentration in the solution, q_{max} (mg g^{-1}) is the maximum adsorption of NH_4^+ ions and K_L (L mg^{-1}) is the Langmuir constant related to the enthalpy of the process. This isotherm is applicable under the following hypothesis: the adsorbent has a uniform surface; absence of interactions between the adsorbent molecules; the adsorption process takes place in a single layer. q_{max} and K_L constants are calculated from the slope and intercept of the plot of C_e/q_e versus C_e, respectively.

The essential feature of the Langmuir isotherm can be expressed by means of dimensionless constant separation factor (R_L), which is calculated using

$$R_L = \frac{1}{1 + K_L C_0} \quad (5)$$

where K_L denotes the Langmuir constant and C_0 is the initial concentration. The R_L parameter is separation factor and is considered as more reliable indicator of the adsorption. There are four probabilities for the R_L value: (i) for favorable adsorption, $0 < R_L < 1$; (ii) for unfavorable adsorption, $R_L > 1$; (iii) for linear adsorption, $R_L = 1$; (iv) for irreversible adsorption, $R_L = 0$ [24].

The Langmuir plots for ammonium adsorption onto NaA zeolite are obtained (Fig. 10a), and the parameters are shown in Table 1. The experimental data fits the Langmuir model well with the correlation coefficient 0.9596. The maximum adsorption capacity is 44.3 mg g^{-1} deduced from Langmuir isotherm. The R_L parameter lies between 0 and 1, which represents that the removal of NH_4^+ by NaA zeolite is favorable. In addition, the values of separation factor (R_L) prove that the NaA zeolite is a potential adsorbent for NH_4^+ removal from aqueous solution.

Several other low-cost absorbents have been used for ammonium ions removal in the literature and their adsorption capacities have also been obtained. For example, Jha and Hayashi [25] reported that the maximum adsorption capacities of NH_4^+ by natural and modified clinoptilolite zeolite were 12.5, 16.1 and 19.5 mg g^{-1} (0.89, 1.15, 1.39 mmol g^{-1}), respectively. Weatherley and Miladinovic [26] found the maximum adsorption capacity of NH_4^+ by New Zealand clinoptilolite and mordenite to be 6.588 and 9.479 mg g^{-1}, respectively. Compared with the results above for NH_4^+ ions removal, it is obvious that the as-synthesized NaA zeolite from halloysite has a relatively higher adsorption capacity. Though the maximum adsorption capacity is based on experimental data from the small scale test, we believe that the as-synthesized NaA zeolite can be used in the practical wastewaters.

The linear form of Freundlich equation is given as:

$$\log q_e = \log K_F + \frac{1}{n}\log C_e \quad (6)$$

where K_F (mg$^{1-1/n}$ L$^{1/n}$ g^{-1}) is Freundlich constant related to the adsorption capacity, C_e (mg L^{-1}) is the concentration in solution, and n is an empirical parameter related to the intensity of adsorption, which varies with the heterogeneity of the material. Higher value for K_F indicates higher affinity for NH_4^+ ions and the value of the empirical parameter $1/n$ lies between $0.1 < 1/n < 1$, indicating favorable adsorption [27]. Freundlich constants are calculated from the slope and intercept of Fig. 10b and are given in Table 1. The correlation coefficient 0.9901 reflects that the experimental data agrees with the Freundlich model. The value of $1/n$ 0.625 for 288 K is smaller than 1 and it represents the favorable removal conditions.

In order to quantitatively compare the applicability of each model, a standard deviation (*SD*) is calculated [28]. As can be seen from Table 1, the values of *SD* from both isotherm models are smaller than 0.500, this further indicates that both Langmuir and Freundlich models fit well with the experimental data.

3.7. Effect of competitive cations

Since industrial effluents are always contaminated by various additives such as inorganic salts, it is important to study the effect

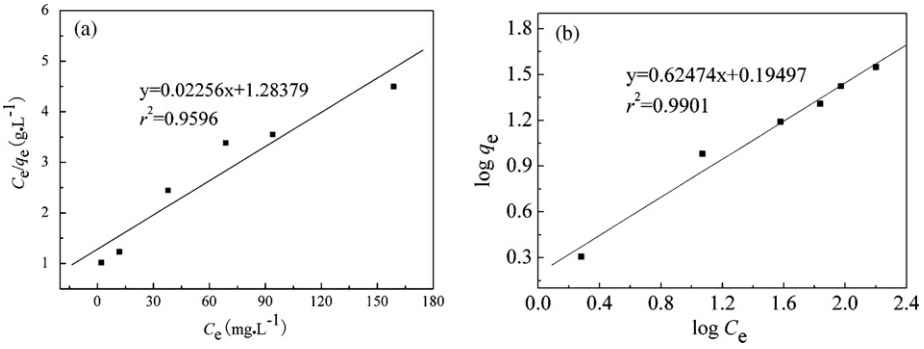

Fig. 10. Isotherm models for ammonium adsorption on NaA zeolite at 288 K (a) Langmuir model and (b) Freundlich model.

Table 1
Isotherm constants for NH_4^+ adsorption on NaA zeolite at 288 K.

Isotherm models	Parameters			
Langmuir	K_L (L mg^{-1}): 0.0176	q_{max} (mg g^{-1}): 44.3	*SD*: 0.433	R_L: 0.159–0.850
Freundlich	K_F (mg$^{1-1/n}$ L$^{1/n}$ g^{-1}): 1.57	1/*n*: 0.625	*SD*: 0.0701	

of these ions on the adsorption property of NH_4^+ solutions. Therefore, the adsorption of NH_4^+ in the presence of salt was carried out at 0.001–0.100 mol L^{-1} sodium (Na^+), potassium (K^+), calcium (Ca^{2+}) and magnesium (Mg^{2+}) ions concentrations, 0.2 g adsorbent and constant initial NH_4^+ concentration of 100 mg L^{-1} at 288 K, respectively. The results are summarized in Table 2. The adsorption capacities of NH_4^+ on NaA zeolite are significantly reduced by the presence of competitive cations. As demonstrated in Table 2, when the concentration of Na^+, K^+, Ca^{2+} and Mg^{2+} increased from 0 (with NH_4^+ only) to 0.100 mol L^{-1}, the NH_4^+ adsorption capacities decreased from 22.06 to 0.50, 0.51, 0.56 and 7.66 mg g^{-1}, respectively.

The adsorption of NH_4^+ on NaA zeolite is due to the ion exchange reaction between NH_4^+ from aqueous solutions and Na^+ from NaA zeolite, which can be expressed as:

$$Z^-\text{–}Na^+ + NH_4^+ \rightleftharpoons Z^-\text{–}NH_4^+ + Na^+ \quad (7)$$

where Z^- symbolizes the negatively charged functional group of the zeolite. As the Na^+ in the solution increased, the reaction would be shifted from the right to the left, resulting in the reduction of NH_4^+ adsorption. When K^+, Ca^{2+} or Mg^{2+} was individually presented in the solution, the adsorption capacity decreased due to the competition with other cations for adsorption on the zeolite, and this competition increases with increase in the starting concentration of other cations. In addition, the effect of competition has an order of $Na^+ > K^+ > Ca^{2+} > Mg^{2+}$ for the same initial cation concentrations. Similar result has also been previously reported by Lei et al. [5].

3.8. Thermodynamic parameters

In order to gain an insight into the mechanism involved in the adsorption process, thermodynamic parameters for the present system are calculated. The adsorption free energy (ΔG^0), adsorption enthalpy (ΔH^0) and adsorption entropy (ΔS^0) at different temperatures (288, 298, 308 K) are calculated using the following equations:

$$\Delta G^0 = -RT \ln K_L \quad (8)$$

$$\Delta G^0 = \Delta H^0 - T\,\Delta S^0 \quad (9)$$

where K_L is the Langmuir constant when concentration terms are expressed in L mol^{-1}, R (8.314 J mol^{-1} K^{-1}) is the universal gas constant and T (K) is the temperature.

ΔH^0 and ΔS^0 are calculated from the intercept and slope of linear plot of ΔG^0 versus T. The values of ΔG^0, ΔH^0 and ΔS^0 parameters are summarized in Table 3. Change in the standard free energy ΔG^0 have negative values, −1.32, −1.21 and −1.05 kJ mol^{-1} at 288, 298 and 308 K, respectively. These results indicate that ammonium adsorption by NaA zeolite is spontaneous and has physical characteristic. Change in the standard enthalpy ΔH^0 value is −5.22 kJ mol^{-1}, indicating that NH_4^+ adsorption is an exothermic process. The negative value of the standard entropy change ΔS^0 (−0.0135 kJ mol^{-1} K^{-1}) suggests that randomness decreases the removal of NH_4^+ on NaA zeolite.

Table 2
Effect of competitive cations for NH_4^+ adsorption on synthesized NaA zeolite at 288 K.

	NH_4^+ adsorption capacity (mg g^{-1})			
NH_4^+ only	22.06			
Cations C_0 (mol L^{-1})	Na^+	K^+	Ca^{2+}	Mg^{2+}
0.001	14.02	14.15	14.43	16.27
0.01	6.83	7.04	10.45	13.47
0.1	0.50	0.51	0.56	7.658

Table 3
Thermodynamic parameters for NH_4^+ adsorption on NaA zeolite.

	Temperature (K)		
	288	298	308
ΔG^0 (kJ mol^{-1})	−1.32	−1.21	−1.05
ΔH^0 (kJ mol^{-1})		−5.22	
ΔS^0 (kJ mol^{-1} K^{-1})		−0.0135	

Table 4
Data about adsorption and regeneration of NaA zeolite.

	Number of cycles						
	1	2	3	4	5	6	7
NH_4^+ adsorption capacity (mg g^{-1})	16.72	16.61	16.53	16.47	16.49	16.39	16.35

3.9. Evaluation of regeneration and reusable ability

A fine adsorbent, in addition to its high adsorption capacity, must also exhibit good regeneration ability for possible reuse. In this study, adsorption experiments were performed using 0.2 g NaA zeolite and 50 mL 100 mg L^{-1} NH_4^+ at 288 K for 30 min, and desorption of adsorbed NH_4^+ onto NaA zeolite was studied using 100 mL 1 mol L^{-1} NaCl solution as the eluent at 288 K for 30 min, and consecutive adsorption–desorption cycles were repeated six times. The results were shown in Table 4. There was a slight decrease in adsorption capacity from 16.72 mg g^{-1} for the first cycle to 16.35 mg g^{-1} for the seventh cycle. This showed the adsorption capacity was almost constant and in accordance with that of the original NaA zeolite.

The results also indicated that 1 mol L^{-1} NaCl solution can act as not only desorbing agent, but also regenerating agent, which made desorption of NH_4^+ and regeneration of NaA zeolite performed simultaneously. So the operation could be simplified and the cost could be cut down. In addition, the simultaneous desorption and regeneration can be completed at room temperature within 30 min, a mild condition. Therefore we believe NaA zeolite could be considered as a good adsorbent for NH_4^+.

4. Conclusion

In conclusion, pure form, single phase and highly crystalline NaA zeolite was successfully synthesized from natural halloysite mineral by hydro-thermal method at moderate conditions. NaA zeolite has exhibited fast adsorption rate and high adsorption capacity to NH_4^+. A maximum adsorption capacity of 44.3 mg g^{-1} of NH_4^+ was achieved. It is higher than other low-cost adsorbents reported for NH_4^+ removal. Both Langmuir and Freundlich models fit well with the experimental data. R_L value from Langmuir isotherm model and 1/*n* from Freundlich isotherm model indicate that the removal of NH_4^+ on the NaA zeolite is favorable. The negative values of ΔG^0

and ΔH^0 show that the adsorption is a spontaneous and exothermic process. The negative value of ΔS^0 indicates the randomness decreases the uptake of NH_4^+ on the NaA zeolite. The regeneration condition of this adsorbent is mild, and the adsorption capacity of the recovered adsorbent is almost constant and in accordance with that of the original adsorbent. Based on the results, it is concluded that the as-prepared NaA zeolite from halloysite can be used as low-cost and relatively effective adsorbent for the removal of NH_4^+ from wastewaters.

Acknowledgements

This work was supported by the National Natural Science Foundation of China (No. 20871105) and Henan Outstanding Youth Science Fund (No. 0612002400).

References

[1] D.J. Randall, T.K.N. Tsui, Ammonia toxicity in fish, Mar. Pollut. Bull. 45 (2002) 17–23.
[2] I. Vazquez, J. Rodriguez, E. Maranon, L. Castrillon, Y. Fernandez, Simultaneous removal of phenol, ammonium and thiocyanate from coke wastewater by aerobic biodegradation, J. Hazard. Mater. B137 (2006) 1773–1780.
[3] A. Manipura, V.L. Barbosa, J.E. Burgess, Comparison of biological ammonium removal from synthetic metal refinery wastewater using three different types of reactor, Miner. Eng. 20 (2007) 617–620.
[4] G. Zaitsev, T. Mettanen, J. Langwaldt, Removal of ammonium and nitrate from cold inorganic mine water by fixed-bed biofilm reactors, Miner. Eng. 21 (2008) 10–15.
[5] L.C. Lei, X.J. Li, X.W. Zhang, Ammonium removal from aqueous solutions using microwave-treated natural Chinese zeolite, Sep. Purif. Technol. 58 (2008) 359–366.
[6] Y.F. Wang, F. Lin, W.Q. Pang, Ion exchange of ammonium in natural and synthesized zeolites, J. Hazard. Mater. 160 (2008) 371–375.
[7] H. Zheng, L.J. Han, H.W. Ma, Y. Zhen, H.M. Zhang, D.H. Liu, S.P. Liang, Adsorption characteristics of ammonium ion by zeolite 13X, J. Hazard. Mater. 158 (2008) 577–584.
[8] E. Maranon, M. Ulmanu, Y. Fernandez, I. Anger, L. Castrillon, Removal of ammonium from aqueous solutions with volcanic tuff, J. Hazard. Mater. 137 (2006) 1402–1409.
[9] P. Vassileva, P. Tzvetkova, R. Nickolov, Removal of ammonium ions from aqueous solutions with coal-based activated carbons modified by oxidation, Fuel 88 (2008) 387–390.
[10] E. Okoniewska, J. Lach, M. Kacprzak, E. Neczaj, The removal of manganese, iron and ammonium nitrogen on impregnated activated carbon, Desalination 206 (2007) 251–258.
[11] M. Sarioglu, Removal of ammonium from municipal wastewater using natural Turkish (Dogantepe) zeolite, Sep. Purif. Technol. 41 (2005) 1–11.
[12] K. Saltali, A. Sari, M. Aydin, Removal of ammonium ion from aqueous solution by natural Turkish (Yildizeli) zeolite for environmental quality, J. Hazard. Mater. 141 (2007) 258–263.
[13] Y.F. Wang, F. Lin, W.Q. Pang, Ammonium exchange in aqueous solution using Chinese natural clinoptilolite and modified zeolite, J. Hazard. Mater. 142 (2007) 160–164.
[14] M. Sprynskyy, M. Lebedynets, R. Zbytniewski, J. Namiesnik, B. Buszewski, Ammonium removal from aqueous solution by natural zeolite, Transcarpathian mordenite, kinetics, equilibrium and column tests, Sep. Purif. Technol. 46 (2005) 155–160.
[15] X. Querol, N. Moreno, J.C. Umana, A. Alastuey, E. Hernandez, A. Lopez-Soler, F. Plana, Synthesis of zeolites from coal fly ash: an overview, Int. J. Coal Geol. 50 (2002) 413–423.
[16] M.A. Saada, M. Soulard, J. Patarin, R.C. Regis, Synthesis of zeolite materials from asbestos wastes: an economical approach, Micropor. Mesopor. Mater. 122 (2009) 275–282.
[17] R. Juan, S. Hernandez, J.M. Andres, C. Ruiz, Ion exchange uptake of ammonium in wastewater from a sewage treatment plant by zeolitic materials from fly ash, J. Hazard. Mater. 161 (2009) 781–786.
[18] D.Y. Wu, B.H. Zhang, C.J. Li, Z.J. Zhang, H.N. Kong, Simultaneous removal of ammonium and phosphate by zeolite synthesized from fly ash as influenced by salt treatment, J. Colloid Interface Sci. 304 (2006) 300–306.
[19] H. Youssef, D. Ibrahim, S. Komarneni, Microwave-assisted versus conventional synthesis of zeolite A from metakaolinite, Micropor. Mesopor. Mater. 115 (2008) 527–534.
[20] D.I. Petkowicz, R.T. Rigo, C. Radtke, S.B. Pergher, J.H.Z. dos Santos, Zeolite NaA from Brazilian chrysotile and rice husk, Micropor. Mesopor. Mater. 116 (2008) 548–554.
[21] Y.M. Lvov, D.G. Shchukin, H. Mohwald, R.R. Price, Halloysite clay nanotubes for controlled release of protective agents, ACS Nano 2 (2008) 814–820.
[22] P. Luo, Y.F. Zhao, B. Zhang, J.D. Liu, Y. Yang, J.F. Liu, Study on the adsorption of Neutral Red from aqueous solution onto halloysite nanotubes, Water Res., doi:10.1016/j.watres.2009.10.042, in press.
[23] C.A. Rios, C.D. Williams, M.A. Fullen, Nucleation and growth history of zeolite LTA synthesized from kaolinite by two different methods, Appl. Clay Sci. 42 (2009) 446–454.
[24] V.K. Gupta, A. Mittal, A. Malviya, J. Mittal, Adsorption of carmoisine A from wastewater using waste materials—bottom ash and deoiled soya, J. Colloid Interface Sci. 335 (2009) 24–33.
[25] V.K. Jha, S. Hayashi, Modification on natural clinoptilolite zeolite for its NH_4^+ retention capacity, J. Hazard. Mater. 169 (2009) 29–35.
[26] L.R. Weatherley, N.D. Miladinovic, Comparison of the ion exchange uptake of ammonium ion onto New Zealand clinoptilolite and mordenite, Water Res. 38 (2004) 4305–4312.
[27] C. Raji, T.S. Anirudhan, Batch Cr (VI) removal by polyacrylamide-grafted sawdust: kinetics and thermodynamics, Water Res. 32 (1998) 3772–3780.
[28] I.A. Sengil, M. Ozacar, H. Turkmenler, Kinetic and isotherm studies of Cu(II) biosorption onto valonia tannin resin, J. Hazard. Mater. 162 (2009) 1046–1052.